

## Landscape of Two-Proton Radioactivity

E. Olsen,<sup>1,2</sup> M. Pfützner,<sup>3,4</sup> N. Birge,<sup>1,2</sup> M. Brown,<sup>1,5</sup> W. Nazarewicz,<sup>1,2,3</sup> and A. Perhac<sup>1,2</sup>

<sup>1</sup>*Department of Physics and Astronomy, University of Tennessee, Knoxville, Tennessee 37996, USA*

<sup>2</sup>*Physics Division, Oak Ridge National Laboratory, Oak Ridge, Tennessee 37831, USA*

<sup>3</sup>*Faculty of Physics, University of Warsaw, ul. Hoża 69, 00-681 Warsaw, Poland*

<sup>4</sup>*CERN, Physics Department, 1211 Geneva 23, Switzerland*

<sup>5</sup>*Physics Department, Berea College, Berea, Kentucky 40404, USA*

(Received 4 March 2013; published 29 May 2013)

Ground-state two-proton ( $2p$ ) radioactivity is a decay mode found in isotopes of elements with even atomic numbers located beyond the two-proton drip line. So far, this exotic process has been experimentally observed in a few light- and medium-mass nuclides with  $Z \leq 30$ . In this study, using state-of-the-art nuclear density functional theory, we globally analyze  $2p$  radioactivity and for the first time identify  $2p$ -decay candidates in elements heavier than strontium. We predict a few cases where the competition between  $2p$  emission and  $\alpha$  decay may be observed. In nuclei above lead, the  $\alpha$ -decay mode is found to be dominating and no measurable candidates for the  $2p$  radioactivity are expected.

DOI: [10.1103/PhysRevLett.110.222501](https://doi.org/10.1103/PhysRevLett.110.222501)

PACS numbers: 21.60.Jz, 23.50.+z, 21.10.Dr, 21.10.Tg

*Introduction.*—With the impressive progress in mapping new territories in the nuclear landscape, new phenomena emerge in rare isotopes with extreme proton-to-neutron imbalance. On the proton-rich side, due to the presence of the Coulomb barrier that has a confining effect on the nucleonic density, relatively long-lived proton emitters exist beyond the proton drip line [1–3]. In recent decades, the phenomenon of proton emission from odd- $Z$  nuclei developed into a powerful spectroscopic tool yielding a wealth of detailed structural information (see the recent review [1] and references quoted therein). In favorable conditions [4], unbound even- $Z$  nuclei may undergo a simultaneous emission of two protons, i.e., exhibit  $2p$  radioactivity. In such cases, due to proton pairing, the emission of a single proton is energetically forbidden or strongly suppressed. The ground-state  $2p$  radioactivity was experimentally discovered in  $^{45}\text{Fe}$  [5,6] and, later on, in  $^{19}\text{Mg}$  [7],  $^{48}\text{Ni}$  [8], and  $^{54}\text{Zn}$  [9]. The interest in the phenomenon of  $2p$  radioactivity has been boosted significantly by the measurement of proton-proton correlations in the decay of  $^{45}\text{Fe}$  [10] that has revealed the three-body character of the process and the sensitivity to the angular momentum composition of the wave function. These findings were corroborated by the recent study of  $2p$  correlations in the decay of  $^6\text{Be}$  resonances [11].

One may ask whether the ground-state  $2p$  radioactivity is limited to just a narrow range of light- and medium-mass nuclei or whether it can also be expected in heavy systems. No detailed predictions, however, have been made for elements heavier than strontium. Most of the previous theoretical estimates were focused on a rather narrow range of nuclei with  $22 < Z < 30$  [12–15] and aimed at identifying the best candidates for initial experimental observations. Motivated by astrophysical applications, these studies were subsequently extended to the region

$30 < Z < 38$  [16]. In almost all of these papers, one- and two-proton separation energies of  $T_z = -T$  nuclei were accurately determined (up to  $\sim 100$  keV) by calculating the Coulomb displacement energies in combination with known experimental masses of mirror  $T_z = T$  systems. The only exception is Ref. [13] where self-consistent mean-field theory with various effective interactions was employed.

The main objective of this work is to delineate for the first time the full landscape of  $2p$  radioactivity. To this end, we use separation energies predicted by large-scale mass table calculations using state-of-the-art nuclear density functional theory (DFT) [17] with several Skyrme energy density functionals (EDFs). In our global survey, we consider all even- $Z$  elements with  $Z \geq 18$ . To estimate half-lives, we use two models of  $2p$  emission: a direct-decay model and a diproton model. In addition, we take into account the competition between  $2p$  emission and  $\alpha$  decay. Although our method is less precise than the approach based on Coulomb displacement energies, it is well suitable for a large-scale, qualitative survey of the  $2p$  emission phenomenon undertaken here.

*Models.*—The nuclear binding energies  $B(Z, N)$  were obtained in the deformed DFT calculations of Refs. [18,19] using six effective Skyrme interaction models in the particle-hole channel (SkM\* [20], SkP [21], SLy4 [22], SV-min [23], UNEDF0 [24], and UNEDF1 [25]) augmented by the density-dependent, zero range pairing term. The binding energies of even-even nuclei across the mass table were calculated by solving the self-consistent Hartree-Fock-Bogoliubov (HFB) equations using the solver HFBTHO [26]. To approximately restore the particle number symmetry broken in HFB, we used the variant of the Lipkin-Nogami scheme formulated in Ref. [27]. The binding energies for odd- $N$

isotopes were determined by adding computed average pairing gaps to the binding energy of the corresponding zero-quasiparticle vacuum obtained by averaging binding energies of even-even neighbors. Considering the uncertainties of current approaches to odd-even binding energy differences [28], this is a reasonable procedure.

The single-particle basis consisted of harmonic oscillator states originating in 20 major oscillator shells. While the proton chemical potential  $\lambda_p$  is positive for proton unbound nuclei, the HFB results obtained with the discretized continuum are very stable in the considered range of binding energies. This is because the Coulomb barrier tends to confine the proton density in the nuclear interior and effectively pushes the continuum up in energy [29,30] on the proton-rich side. As discussed in Ref. [18], because of the Coulomb effect, the proton drip line lies relatively close to the valley of stability; hence, the associated model extrapolation error is small. Indeed all the models we use are very consistent when it comes to the prediction of the two-proton drip line; see Fig. 1.

The half-lives for  $2p$  decay were estimated using two simple models. The first, direct-decay model, results from the factorization of the decay amplitude into a product of two-body terms [31]. The removal of one proton leaves the core +  $p$  system in a state of energy  $E_p$ , relative to the

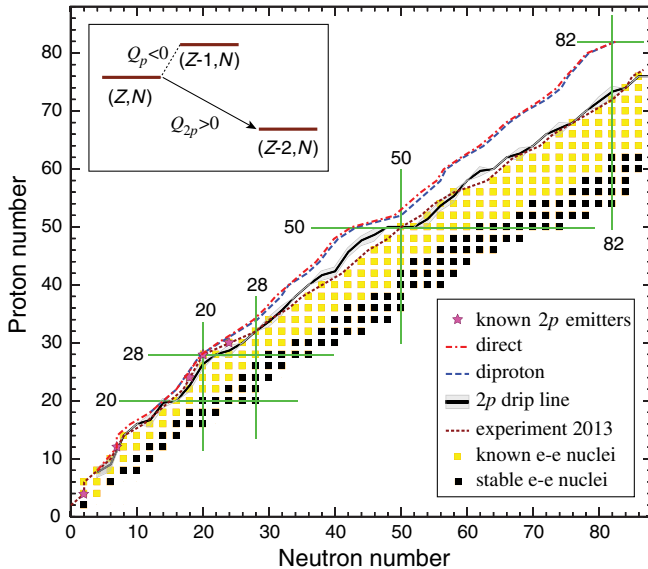


FIG. 1 (color online). The landscape of ground-state  $2p$  emitters. The mean two-proton drip line (thick black line) and its uncertainty (gray) were obtained in Ref. [18] by averaging the results of six interaction models. The known proton-rich even-even nuclei are marked by yellow squares, stable even-even nuclei by black squares, and known  $2p$  emitters by stars. The current experimental reach for even- $Z$  nuclei (including odd- $A$  systems) [37] is marked by a dotted line. The average lines  $N_{av}(Z)$  of  $2p$  emission for the diproton model (dashed line) and direct-decay model (dash-dotted line) are shown. The energetic condition (1) for the true  $2p$  decay is illustrated in the inset.

three-body decay threshold, and requires a transfer of orbital angular momentum  $l_p$ . The core +  $p$  system is taken here as the ground state of the one-proton daughter; hence,  $E_p = Q_{2p} - Q_p$ , where  $Q_{2p}$  and  $Q_p$  denote the decay energies for  $2p$  and single-proton emission, respectively. All calculations in this global survey were made with  $l_p = 0$ , i.e., assuming the fastest decay possible. In this way, we establish a limit of the least neutron-deficient nuclei decaying by  $2p$  emission. We note, however, that inclusion of larger values of angular momentum, in particular,  $l_p = 1$ , known to occur around  $Z = 28$ , would increase the number of predicted candidates. The direct-decay widths were calculated using the version of the model given by Eq. (20) of Ref. [3] with the spectroscopic factor  $\theta^2$  determined by comparison with the experimentally established four  $2p$  emitters shown in Table I. Using the experimental separation energies, the average value  $\theta^2 = 0.173$  was obtained that gives a very reasonable agreement with experiment, see Table I, and has been used in subsequent calculations of half-lives:  $T_{2p} = \hbar \ln 2 / \Gamma_{2p}$ .

The diproton model assumes that both protons leave the core nucleus as a correlated  $2p$  pair with  $l = 0$ . Within this model [12,13], the  $2p$ -decay width is given by the Wentzel-Kramers-Brillouin expression. In our calculations, the average diproton potential has been approximated by  $2V_p(r)$ , where  $V_p$  is the average proton potential containing the Woods-Saxon field in the Chepurinov parametrization [32] and the Coulomb term. (The results are fairly insensitive to the choice of the average potential [13].) The diproton spectroscopic factor can be estimated in the cluster overlap approximation [12]:  $\theta_{dipr}^2 = G^2 [A/(A-2)]^{2n} \mathcal{O}^2$ , where  $G^2 = (2n)! / [2^{2n} (n!)^2]$  [33],  $\mathcal{O}^2$  is the proton overlap function, and  $n$  is the average principal proton oscillator quantum number given by  $n \approx (3Z)^{1/3} - 1$  [34]. The value of  $\mathcal{O}^2 = 0.015$  was determined by a  $\chi^2$  optimization to the experimental half-lives of  $^{19}\text{Mg}$ ,  $^{45}\text{Fe}$ ,  $^{48}\text{Ni}$ , and  $^{54}\text{Zn}$ . The values of half-lives for these nuclei predicted by the diproton model are given in Table I; they are consistent with the direct-decay model and the estimates of Refs. [31,35].

To determine the competition between  $2p$  and  $\alpha$  decay, the  $2p$ -decay half-lives were compared to  $\alpha$ -decay half-lives obtained from the global phenomenological expression of Ref. [36].

TABLE I. Experimental partial  $2p$  half-lives used to optimize the spectroscopic factors and the resulting predictions of the direct-decay and diproton models. In the direct model,  $l_p = 0$  was assumed.

Nucleus	Experiment	Direct	Diproton
$^{19}\text{Mg}$ [7]	4.0(15) ps	6.2 ps	12.3 ps
$^{45}\text{Fe}$ [10]	3.7(4) ms	1.1 ms	8.7 ms
$^{48}\text{Ni}$ [8]	$3.0^{+2.2}_{-1.2}$ ms	6.8 ms	5.3 ms
$^{54}\text{Zn}$ [9]	$1.98^{+0.73}_{-0.41}$ ms	1.0 ms	0.8 ms

*Selection criteria.*—The candidates for  $2p$  decay were selected according to the energy criterion:

$$Q_{2p} = -S_{2p} > 0, \quad Q_p = -S_p < 0, \quad (1)$$

where  $S_p = B(Z-1, N) - B(Z, N)$  and  $S_{2p} = B(Z-2, N) - B(Z, N) \approx -2\lambda_p$  are the one- and two-proton separation energies, respectively. The condition (1) corresponds to true  $2p$  decay as the simultaneous emission of two protons; the sequential emission of two protons is energetically impossible (see the inset in Fig. 1). For the EDFs used in this work, the rms deviation from the experimental  $S_{2p}$  values is typically less than 1 MeV. For instance, for UNEDF0 and UNEDF1, it is 0.86 and 0.79 MeV, respectively [25].

In addition to the energy constraint (1), we imposed a condition on  $2p$  decay half-lives:

$$10^{-7} \text{ s} < T_{2p} < 10^{-1} \text{ s}, \quad (2)$$

which defines the feasibility of experimental observation of the  $2p$  decay. The lower bound of 100 ns corresponds to the typical sensitivity limit of in-flight, projectile-fragmentation techniques [3]. The upper bound of 100 ms ensures that the  $2p$  decay will not be dominated by  $\beta$  decay. (We note that the half-lives of the observed medium-mass  $2p$  emitters are all in the range of several ms.) Moreover, to eliminate the fast  $\alpha$  emitters from our considerations, we only considered cases satisfying

$$T_{2p} < 10T_\alpha. \quad (3)$$

This condition guarantees that the  $2p$ -decay branch is at least 10%. Of these candidates, to select the cases where the competition between  $2p$  and  $\alpha$  decay can be seen, we used the criterion  $0.1T_{2p} < T_\alpha < 10T_{2p}$ , which ensures that the branching ratio for  $2p$  or  $\alpha$  decay is at least 10%.

*Results.*—For each model considered in this work, we selected candidates for  $2p$  emission according to the imposed criteria on lifetimes (2) and (3). We define the model multiplicity  $m(Z, N) = k$  if a nucleus  $(Z, N)$  is predicted by  $k$  models ( $k = 1, \dots, 6$ ) to be a  $2p$  emitter. The average path for the  $2p$  emission in the  $(Z, N)$  plane is given by  $N_{\text{av}}(Z)$ , where—for a given element  $Z$ —the model-averaged neutron number is  $N_{\text{av}}(Z) = \sum_N N m(Z, N) / \sum_N m(Z, N)$ , provided that at least one candidate has been found for this  $Z$ . Figure 1 shows the trajectories  $N_{\text{av}}(Z)$  for both the direct-decay and diproton models. It is seen that (i) both ways of estimating  $2p$  half-lives give very similar predictions for the average path of  $2p$  radioactivity and that (ii) this path quickly departs from the two-proton drip line with increasing atomic number. Furthermore, according to our calculations,  $\alpha$  decays win over  $2p$  emission above lead, so  $Z = 82$  marks the upper border of the ground-state  $2p$  emission landscape. The intermodel consistency for the predicted  $Q_{2p}$  values along  $N_{\text{av}}(Z)$  is good; namely, the rms deviation for our six EDFs

is typically 150 keV, i.e., well below the average deviation from experiment.

Results of our survey are presented in more detail in Fig. 2. We see that each element between nickel and lead has isotopes predicted to undergo  $2p$  radioactivity. In the case of xenon ( $Z = 54$ ), all  $2p$ -decaying candidates are found to be dominated by  $\alpha$  decay in the diproton model;  $^{105}\text{Xe}$  is predicted to be a  $2p$  emitter by the direct-decay model. For three light elements ( $Z = 20, 24, 26$ ), no  $2p$  candidates are predicted because the calculated half-lives were shorter than the lower limit of condition (2), which is a consequence of our restriction to the  $l = 0$  decay channel. We note that the observed  $2p$  decay of  $^{45}\text{Fe}$  is dominated by the  $l = 1$  channel [3]. While the nuclei  $^{54}\text{Zn}$ ,  $^{59}\text{Ge}$ ,  $^{63}\text{Se}$ ,  $^{67}\text{Kr}$ , and  $^{71}\text{Sr}$  discussed in [16] are generally expected to meet the energy criterion (1), their predicted  $Q_{2p}$  values are too low to meet the lifetime criterion (2). In general, due to large uncertainties in the calculated half-lives due to uncertainties in  $Q_{2p}$  [35], the estimated error

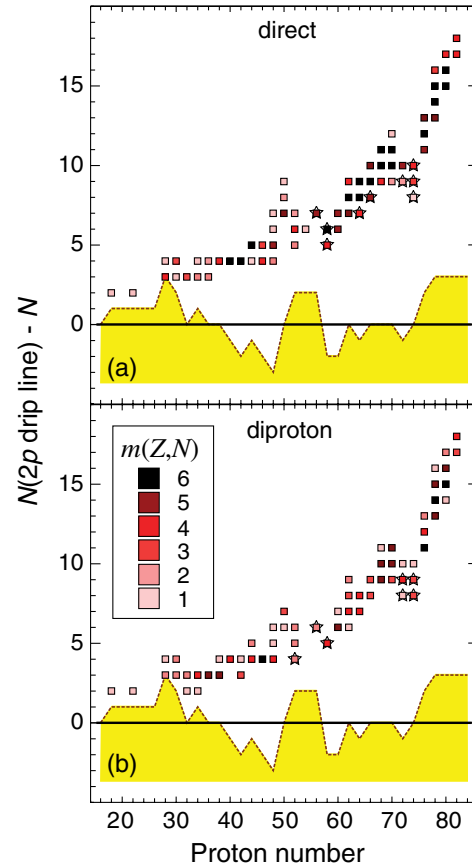


FIG. 2 (color online). The predictions of the direct-decay model (a) and diproton model (b) for the ground-state  $2p$  radioactivity. For each value of  $Z \geq 18$ , neutron numbers  $N$  of predicted proton emitters are shown relative to the average two-proton drip line of Ref. [18] shown in Fig. 1. The model multiplicity  $m(Z, N)$  is indicated by the legend. The candidates for competing  $2p$  and  $\alpha$  decay are marked by stars. The current experimental reach of Fig. 1 is marked by a dotted line.

on the predicted neutron number of a  $2p$  emitter is  $\Delta N = 1$ .

In the region beyond  $^{54}\text{Zn}$ , the predicted  $2p$ -decay candidates which are closest to the current experimental reach are  $^{57,58}\text{Ge}$  (3,2),  $^{62,63}\text{Se}$  (2,1),  $^{66}\text{Kr}$  (3), and  $^{102,103}\text{Te}$  (3,2), where the numbers in parentheses indicate the corresponding number of neutrons beyond the most neutron-deficient isotope known to date. All other cases are located by more than 3 neutrons from the present body of known isotopes. This distance is increasing with increasing atomic number and reaches 14 neutrons for  $^{165}\text{Pb}$ , which is predicted to be the  $2p$  emitting lead isotope closest to the drip line. Other best candidates for ground-state  $2p$  radioactivity in heavy nuclei, according to both direct-decay and diproton models, are  $^{73}\text{Zr}$ ,  $^{77}\text{Mo}$ ,  $^{81}\text{Ru}$ ,  $^{85}\text{Pd}$ ,  $^{113}\text{Ce}$ ,  $^{117}\text{Nd}$ ,  $^{121}\text{Sm}$ ,  $^{125,126}\text{Gd}$ ,  $^{130}\text{Dy}$ ,  $^{133-135}\text{Er}$ ,  $^{138,139}\text{Yb}$ ,  $^{151,152}\text{Os}$ ,  $^{154-156}\text{Pt}$ , and  $^{158,159}\text{Hg}$ . Two nuclei,  $^{155}\text{Pt}$  and  $^{159}\text{Hg}$ , have been consistently predicted to be  $2p$  emitters in all models.

In several cases a competition between  $2p$  and  $\alpha$  decay is predicted. The best candidates, marked in Fig. 2 by a star, are  $^{103}\text{Te}$ ,  $^{109,110}\text{Ba}$ ,  $^{113,114}\text{Ce}$ ,  $^{127}\text{Gd}$ ,  $^{131}\text{Dy}$ ,  $^{144,145}\text{Hf}$ , and  $^{147-149}\text{W}$ . The nuclei  $^{144}\text{Hf}$  and  $^{148,149}\text{W}$  are predicted both in the direct-decay and diproton models, but they are far from the line of the current experimental reach. The closest one is  $^{103}\text{Te}$ , predicted in the diproton model with SkM\* and SLy4 ( $Q_{2p} \approx 3.3$  MeV,  $Q_{\alpha} \approx 4.4$  MeV). (More recently optimized functionals SV-min and UNEDF1 give  $Q_{2p} \approx 2.75$  MeV,  $Q_{\alpha} \approx 3.7$  MeV, i.e., much longer half-lives.)

*Conclusions.*—In this theoretical survey, based on the nuclear DFT, we quantified the landscape of ground-state  $2p$  radioactivity. To assess model-dependent extrapolations beyond the two-proton drip line, we applied six models based on Skyrme EDFs and two approaches to  $2p$  half-lives. Our results provide a consistent picture of the  $2p$  radioactivity. Most importantly, we find that this decay mode is not an isolated phenomenon, limited to a narrow range of light- and medium-mass nuclei, but a typical feature for the proton-unbound isotopes with even atomic numbers. According to our calculations, almost all elements between argon and lead have  $2p$ -decaying isotopes. The upper end of the  $2p$ -decay territory is determined by  $\alpha$  decay, which totally dominates above  $Z = 82$ . Unfortunately, most of the new candidates for the  $2p$  radioactivity are located far beyond the current experimental reach. Only in two regions is the  $2p$ -decay mode predicted to occur close enough to be addressed by today's experiments. One ranges from germanium to krypton, and the second region is located just above tin. Other regions will have to wait for the facilities of the next generation. A confrontation of our predictions for heavier  $2p$  emitters with the future data will be of great value for modeling of proton-unstable nuclei and improving the nuclear EDF.

Perhaps the most interesting are nuclei around  $^{103}\text{Te}$ – $^{110}\text{Ba}$ , in which the competition between  $2p$

emission and  $\alpha$  decay is predicted. The observation of these two decay modes in the same nucleus would provide an excellent test of nuclear structure models and a deeper understanding of the dynamics of charged particle emission from nuclei. Finally, we note that all EDFs employed in our study, including the traditional ones (SkM\*, SkP, SLy4) as well as the recently optimized ones (SV-min, UNEDF0, UNEDF1), yield a similar range of  $2p$  radioactivity: while details for individual nuclei differ because of high sensitivity of  $2p$  and  $\alpha$ -decay half-lives to predicted  $Q$  values, the global trends presented in this survey seem to be fairly robust.

This work was supported by the U.S. Department of Energy (DOE) under Contracts No. DE-FG02-96ER40963 (University of Tennessee), No. DE-FG52-09NA29461 (the Stewardship Science Academic Alliances program), and No. DE-SC0008499 (NUCLEI SciDAC Collaboration), and by the Polish National Science Center under Contract No. DEC-2011/01/B/ST2/01943. Computer time was provided by the INCITE program. This research used resources of the OLCF facility, which is supported by the DOE under Contract No. DE-AC05-00OR22725.

- 
- [1] M. Pfützner, M. Karny, L. Grigorenko, and K. Riisager, *Rev. Mod. Phys.* **84**, 567 (2012).
  - [2] B. Blank and M. Borge, *Prog. Part. Nucl. Phys.* **60**, 403 (2008); B. Blank and M. Płoszajczak, *Rep. Prog. Phys.* **71**, 046301 (2008).
  - [3] M. Pfützner, *Phys. Scr.* **T152**, 014014 (2013).
  - [4] V. Goldansky, *Nucl. Phys.* **19**, 482 (1960).
  - [5] M. Pfützner *et al.*, *Eur. Phys. J. A* **14**, 279 (2002).
  - [6] J. Giovinazzo *et al.*, *Phys. Rev. Lett.* **89**, 102501 (2002).
  - [7] I. Mukha *et al.*, *Phys. Rev. Lett.* **99**, 182501 (2007); *Phys. Rev. C* **77**, 061303(R) (2008).
  - [8] M. Pomorski *et al.*, *Phys. Rev. C* **83**, 061303 (2011).
  - [9] B. Blank *et al.*, *Phys. Rev. Lett.* **94**, 232501 (2005); P. Ascher *et al.*, *Phys. Rev. Lett.* **107**, 102502 (2011).
  - [10] K. Miernik *et al.*, *Phys. Rev. Lett.* **99**, 192501 (2007).
  - [11] L. V. Grigorenko *et al.*, *Phys. Lett. B* **677**, 30 (2009); I. A. Egorova *et al.*, *Phys. Rev. Lett.* **109**, 202502 (2012).
  - [12] B. A. Brown, *Phys. Rev. C* **43**, R1513 (1991).
  - [13] W. Nazarewicz, J. Dobaczewski, T. R. Werner, J. A. Maruhn, P.-G. Reinhard, K. Rutz, C. R. Chinn, A. S. Umar, and M. R. Strayer, *Phys. Rev. C* **53**, 740 (1996).
  - [14] B. J. Cole, *Phys. Rev. C* **54**, 1240 (1996).
  - [15] W. E. Ormand, *Phys. Rev. C* **53**, 214 (1996); **55**, 2407 (1997).
  - [16] B. A. Brown, R. R. C. Clement, H. Schatz, A. Volya, and W. A. Richter, *Phys. Rev. C* **65**, 045802 (2002).
  - [17] M. Bender, P.-H. Heenen, and P.-G. Reinhard, *Rev. Mod. Phys.* **75**, 121 (2003).
  - [18] J. Erler, N. Birge, M. Kortelainen, W. Nazarewicz, E. Olsen, A. Perhac, and M. Stoitsov, *Nature (London)* **486**, 509 (2012).
  - [19] J. Erler, N. Birge, M. Kortelainen, W. Nazarewicz, E. Olsen, A. Perhac, and M. Stoitsov, *J. Phys. Conf. Ser.* **402**, 012030 (2012).



- [20] J. Bartel, P. Quentin, M. Brack, C. Guet, and H.-B. Håkansson, *Nucl. Phys.* **A386**, 79 (1982).
- [21] J. Dobaczewski, H. Flocard, and J. Treiner, *Nucl. Phys.* **A422**, 103 (1984).
- [22] E. Chabanat, P. Bonche, P. Haensel, J. Meyer, and R. Schaeffer, *Nucl. Phys.* **A635**, 231 (1998).
- [23] P. Klüpfel, P.-G. Reinhard, T.J. Bürvenich, and J.A. Maruhn, *Phys. Rev. C* **79**, 034310 (2009).
- [24] M. Kortelainen, T. Lesinski, J. Moré, W. Nazarewicz, J. Sarich, N. Schunck, M. V. Stoitsov, and S. Wild, *Phys. Rev. C* **82**, 024313 (2010).
- [25] M. Kortelainen, J. McDonnell, W. Nazarewicz, P.-G. Reinhard, J. Sarich, N. Schunck, M. V. Stoitsov, and S.M. Wild, *Phys. Rev. C* **85**, 024304 (2012).
- [26] M. Stoitsov, J. Dobaczewski, W. Nazarewicz, and P. Ring, *Comput. Phys. Commun.* **167**, 43 (2005).
- [27] M. V. Stoitsov, J. Dobaczewski, W. Nazarewicz, S. Pittel, and D. J. Dean, *Phys. Rev. C* **68**, 054312 (2003).
- [28] G. F. Bertsch, C. A. Bertulani, W. Nazarewicz, N. Schunck, and M. V. Stoitsov, *Phys. Rev. C* **79**, 034306 (2009).
- [29] J. Dobaczewski, I. Hamamoto, W. Nazarewicz, and J. A. Sheikh, *Phys. Rev. Lett.* **72**, 981 (1994).
- [30] T. Vertse, A. T. Kruppa, and W. Nazarewicz, *Phys. Rev. C* **61**, 064317 (2000).
- [31] L. V. Grigorenko and M. V. Zhukov, *Phys. Rev. C* **68**, 054005 (2003).
- [32] V. A. Chepurnov, *Yad. Fiz.* **7**, 1199 (1968) [*Sov. J. Nucl. Phys.* **7**, 715 (1968)].
- [33] N. Anyas-Weiss *et al.*, *Phys. Rep.* **12**, 201 (1974).
- [34] A. Bohr and B. R. Mottelson, *Nuclear Structure* (W. A. Benjamin, New York, 1969), Vol. 1.
- [35] B. A. Brown and F. C. Barker, *Phys. Rev. C* **67**, 041304(R) (2003).
- [36] H. Koura, *J. Nucl. Sci. Technol.* **49**, 816 (2012).
- [37] M. Thoennessen, *Rep. Prog. Phys.* **76**, 056301 (2013); Discovery of Isotopes Project, <http://www.nsl.msu.edu/~thoenness/isotopes/>.